

# Barriers to Rotation about the B—X Bonds of Coordinatively Unsaturated Borates and Thioborates $R_2BXR'$ (X = O, S) Are Not Measures of the Relative Strengths of Their B=O and B=S $\pi$ Bonds

Michael T. Ashby\* and Nader A. Sheshtawy

Department of Chemistry and Biochemistry, University of Oklahoma,  
Norman, Oklahoma 73019

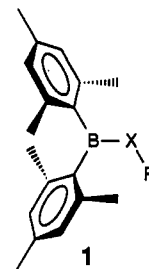
Received August 27, 1993\*

The molecular structures of (2,4,6- $C_6H_2(CH_3)_3$ ) $_2BXCH_3$  (1(X=O,S)) have been determined by single-crystal X-ray crystallography. Derivative 1(X=O) crystallizes in the triclinic space group  $P\bar{1}$  with  $Z = 2$ ,  $a = 8.155(3)$  Å,  $b = 10.230(6)$  Å,  $c = 11.328(5)$  Å,  $\alpha = 65.62(4)^\circ$ ,  $\beta = 72.70(3)^\circ$ ,  $\gamma = 82.12(4)^\circ$ ,  $R = 0.073$ , and  $R_w = 0.083$  at  $-90^\circ$  C. Derivative 1(X=S) crystallizes in the monoclinic space group  $P2_1/c$  with  $Z = 4$ ,  $a = 13.509(8)$  Å,  $b = 8.132(5)$  Å,  $c = 16.079(6)$  Å,  $\beta = 99.66(4)^\circ$ ,  $R = 0.067$ , and  $R_w = 0.089$  at  $25^\circ$  C. The boron atoms adopt approximate trigonal planar geometries, and the XC moieties lie in the  $C_2BX$  planes, an orientation about the B—X bond that maximizes  $Bp\pi-Xp\pi$  bonding. The mesitylene rings are rotated  $\sim 60^\circ$  with respect to the  $C_2BX$  plane, which prohibits significant  $Bp\pi$ -aryl interaction. Thus, the crystal structures of 1(X=O,S) offer benchmarks for comparing discrete  $Bp\pi-Xp\pi$  bonds: B—O =  $1.351(5)$  Å, B—O—C =  $123.6(3)^\circ$ , C—B—O—C =  $173.8(3)^\circ$ , C'—B—O—C =  $-4.0(5)^\circ$ ; B—S =  $1.792(6)$  Å, B—S—C =  $109.4(3)^\circ$ , C—B—S—C =  $175.9(4)^\circ$ , C'—B—S—C =  $-4.3(6)^\circ$ . A comparison of the B and X effective radii (calculated by assuming the B—C and X—C lengths represent single bonds) indicates that the B—O bond is stronger than the B—S bond. *Ab initio* molecular orbital calculations have been carried out on the model compounds  $H_2BXH$  (2(X=O,S)). The geometries of 2 have been optimized at the SCF level for various rotational orientations about the B—X bonds. The ground-state geometries of 2 are analogous to those observed experimentally, with the X—H bonds lying in the trigonal planes of the boron atoms. Mirroring the dynamic behavior observed experimentally, the energy barrier found for rotation about the B—X bond of 2(X=S) is larger than that for 2(X=O). Mulliken population analysis suggests, with respect to the  $BH_2$   $\pi$ -acceptor moiety, that the OH and SH groups are comparable  $\pi$  donors in the ground-state geometry (H—B—X—H =  $0, 180^\circ$ ), but the OH group is a much better  $\pi$  donor than the SH group in the transition-state geometry (H—B—X—H =  $90^\circ$ ). Thus the trend in the barriers to rotation is attributed to a greater stabilization of the transition state by oxygen and not a stronger  $Bp\pi-Sp\pi$  bond in the ground state. Accordingly, rotational barriers about the B—X bonds of  $R_2BOR'$  and  $R_2BSR'$  complexes are not measures of their relative B—X  $\pi$ -bond strengths.

## Introduction

The molecular and electronic structures of compounds that bear multiple bonds that involve one or more of the heavier main group elements have been investigated for several decades.<sup>1</sup> It has been recognized for some time that significant differences exist in the structural and reaction properties of the lighter (first row) and heavier (second-fourth row) congeners.<sup>2</sup> This is no more evident than in the descriptive chemistry of alkoxides and thiolates. Such ligands are capable of stabilizing coordinatively unsaturated atoms via  $\pi$  donation of the chalcogenide lone pair, and considerable effort has focused on assessing their relative  $\pi$ -donor abilities toward both main group and transition metal acceptors. In making such a comparison, it is desirable to have a pair of isomorphous compounds

that contain single donor/acceptor bonds that are not perturbed by substituents that might infer unusual steric or electronic properties. One well-studied system is 1,



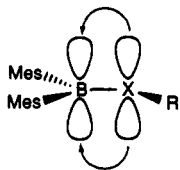
which consists of a 3-coordinate unsaturated (6-electron) borane that is stabilized kinetically by the sterically demanding mesitylene groups and electronically by  $\pi$  donation by the chalcogen X.

The molecular structure of 1 in solution has been the subject of  $^1H$ ,  $^{11}B$ , and  $^{13}C$  NMR studies.<sup>3</sup> Although the orientation of the mesitylene rings remains a controversial point,<sup>3d</sup> it is generally agreed that the XR groups lie in the

\* Abstract published in *Advance ACS Abstracts*, December 1, 1993.  
(1) For recent experimental studies see: (a) Petrie, M. A.; Olmstead, M. M.; Power, P. P. *J. Am. Chem. Soc.* 1991, 113, 8704 and references therein. For theoretical studies involving heavy-atom multiple bonding between C, N, O, Si, P, and S see: (b) Schmidt, M. W.; Truong, P. N.; Gordon, M. S. *J. Am. Chem. Soc.* 1987, 109, 5217 and references therein. Theoretical studies involving multiple bonding between B and heavy main group elements are cited herein.

(2) For a discussion of the origin of these differences see: Kutzelnigg, W. *Angew. Chem., Int. Ed. Engl.* 1984, 23, 272 and references therein.

trigonal  $C_2BX$  plane, an orientation that allows optimum  $Bp\pi-Xp\pi$  bonding:



The dynamic properties of the molecular structures of **1** have also been studied by NMR; of particular interest are the barriers to rotation about the B-X bonds. Remarkably, the barrier to rotation about the B-S bond is substantially greater than the related barrier to rotation about the B-O bond.<sup>2</sup> This has led some workers to the surprising conclusion that the thiolate ligand is a better  $\pi$  donor compared to the alkoxide in this particular system.<sup>3d</sup> In other words, the  $B2p\pi-S3p\pi$  bond is stronger than the  $B2p\pi-O2p\pi$  bond! In the present paper, we describe the molecular structures of a pair of isomorphous organoborate and organothioborate complexes of formula **1**, and we critically review the three factors that have been cited as evidence of  $p\pi-p\pi$  bonding in such compounds: (1) short B-X bond distances, (2) relatively large B-X-R' bond angles, and (3) significant rotational barriers about the B-X bonds.

### Experimental Section

**Syntheses and X-ray Crystallography.** The compound **1** ( $X=O, R=CH_3$ ) was synthesized using Schlenk techniques according to the literature procedure<sup>3a</sup> from dimesitylboron fluoride (Aldrich) and methanol (dried over magnesium). X-ray-quality crystals were grown from saturated pentane (dried over Na/K alloy) solutions at  $-30^\circ C$ . Compound **1** ( $X=S, R=CH_3$ ) was synthesized by a modified procedure<sup>3c</sup> as follows: To diethyl ether (20 mL, dried from Na/K alloy) and Mg (0.25 g, 10.0 mmol) was added dropwise iodomethane (ca. 2 mL, ca. 30 mmol) over a 1-h period. Methyl mercaptan (Aldrich) was bubbled into the solution containing the Grignard. A fine white precipitate of the magnesium thiolate formed. A second Schlenk flask was charged with dimesitylboron fluoride (2.01 g, 7.5 mmol) in a drybox. The slurry of thiolate was added to the dimesitylboron fluoride via large-bore Teflon tubing, and the resulting mixture was allowed to stir overnight. The volatiles were removed under vacuum, and the resulting white solid was extracted with dry pentane. Only a small amount of the solid dissolved. X-ray-quality crystals of **1** ( $X=S, R=CH_3$ ) were grown from the pentane solution upon cooling to  $-30^\circ C$ . Solid samples of **1** ( $X=O, R=CH_3$ ) and **1** ( $X=S, R=CH_3$ ) may be handled in the air for short periods of time. A solution of **1** ( $X=S, R=CH_3$ ) was converted to **1** ( $X=O, R=H$ ) very rapidly upon exposure to atmospheric moisture.

X-ray data were collected with an Enraf-Nonius CAD-4 diffractometer using monochromated Mo  $K\alpha$  radiation ( $\lambda = 0.71069 \text{ \AA}$ ) and methods standard in this laboratory.<sup>4</sup> The crystallographic data are summarized in Table 1. Automatic centering, indexing, and least-squares routines were used to obtain the cell dimensions. The data were collected and corrected for Lorentz and polarization effects;<sup>5</sup> however, no absorption correction was applied since it was judged to be negligible. Crystal integrity was followed by periodically recollecting three reflec-

**Table 1. Crystallographic Data for (2,4,6- $C_6H_2(CH_3)_3$ ) $_2$ BXCH $_3$  ( $1(X=O,S)$ )<sup>a</sup>**

	<b>1(X=O)</b>	<b>1(X=S)</b>
formula	$C_{19}H_{25}BO$	$C_{19}H_{25}BS$
fw	280.22	296.28
color	colorless	colorless
cryst system	triclinic	monoclinic
space group	$P\bar{1}$ (No. 2)	$P2_1/c$ (No. 14)
cell dimens <sup>b</sup>		
<i>a</i> , $\text{\AA}$	8.155(3)	13.509(8)
<i>b</i> , $\text{\AA}$	10.230(6)	8.132(5)
<i>c</i> , $\text{\AA}$	11.328(5)	16.079(6)
$\alpha$ , deg	65.62(4)	
$\beta$ , deg	72.70(3)	99.66(4)
$\gamma$ , deg	82.12(4)	
<i>V</i> , $\text{\AA}^3$	821.7(7)	1741.3(16)
Z	2	4
$\rho_{\text{calc}}$ , $\text{g cm}^{-3}$	1.54	1.50
crystal dimens, mm	$0.37 \times 0.29 \times 0.20$	$0.49 \times 0.28 \times 0.11$
radiation	Mo $K\alpha$ ( $\lambda = 0.71069 \text{ \AA}$ )	Mo $K\alpha$ ( $\lambda = 0.71069 \text{ \AA}$ )
$\mu$ , $\text{mm}^{-1}$	0.072	0.177
temp, K	183	298
data collection	3-53	3-53
range, deg		
no. of unique data	3405	3599
no. of data used ( $I > 2\sigma(I)$ )	2792	1637
$R^c$	0.073	0.067
$R_w^d$	0.083	0.084
final residual, $e \text{ \AA}^{-3}$	0.36	0.30
largest shift/esd, final cycle	0.43	0.04

<sup>a</sup> The standard deviation of the least significant figure is given in parentheses in this and subsequent tables. <sup>b</sup> Obtained from the least-squares refinement of 25 setting angles. <sup>c</sup>  $R = \sum ||F_o| - |F_c|| / \sum |F_o|$ . <sup>d</sup>  $R_w = [\sum w(|F_o| - |F_c|)^2 / \sum w|F_o|^2]^{1/2}$ ;  $w = 1/\sigma^2(F_o)$ .

tions. No decay was observed for **1** ( $X=O, R=CH_3$ ) at  $-90^\circ C$ ; however, a decay of approximately 9% was observed for **1** ( $X=S, R=CH_3$ ) at  $25^\circ C$ . The decay was found to be linear with respect to time and was corrected for using a scaling factor. The structures were solved by direct methods using the SHELX-86<sup>6</sup> program. Refinement of the structures was by full-matrix least-squares calculations using SHELX-76<sup>7</sup> initially with isotropic and finally with anisotropic temperature factors for the non-hydrogen atoms. Neutral-atom scattering factors were used for all atoms.<sup>8</sup> At an intermediate stage of refinement, a difference map revealed maxima consistent with the positions of hydrogen atoms which were included in the subsequent cycles of refinement with isotropic temperature factors the same as those of the carbon atoms to which they are bound. The aromatic hydrogen atoms were allowed to ride in idealized positions. The methyl hydrogen atoms were refined as rotors. Unit weights were used in the early stages of refinement, and weights derived from counting statistics were used in the final cycles of refinement. A difference map calculated at the end of the refinement of **1** ( $X=O, R=CH_3$ ) showed residual peaks that correspond to alternative conformations of the para methyl groups. No attempt was made to model the disorder. A difference map calculated at the end of the refinement of **1** ( $X=S, R=CH_3$ ) showed no chemically significant features.

**Computational Method.** *Ab initio* all-electron calculations were performed using GAMESS.<sup>9</sup> The restricted Hartree-Fock (RHF) method and the 6-31\* polarization basis set were used in all of the calculations involving  $H_2BXH_2$  ( $X=O,S$ ), and  $H_2BXH-NH_3$  ( $4(X=O,S)$ ).<sup>10</sup> Unlike the 6-31\*\* basis set, the 6-31\* basis set contains no provision for polarization of the s orbitals on hydrogen. However, trial calculations using the 6-31\*\* basis set for the GS and TS geometries of  $2(X=O,S)$  indicate the larger

(3) (a) Finocchiaro, P.; Gust, D.; Mialow, K. *J. Am. Chem. Soc.* 1973, 95, 7029. (b) Brown, N. M. D.; Davidson, F.; McMullan, R.; Wilson, J. W. *J. Organomet. Chem.* 1980, 193, 271. (c) Davidson, F.; Wilson, J. W. *J. Organomet. Chem.* 1981, 204, 147. (d) Brown, N. M. D.; Davidson, F.; Wilson, J. W. *J. Organomet. Chem.* 1981, 210, 1.

(4) (a) Khan, M. A.; Taylor, R. W.; Lehn, J. M.; Dietrich, B. *Acta Crystallogr.* 1988, C44, (b) Ashby, M. T.; Khan, M. A.; Halpern, J. *Organometallics* 1991, 10, 2011.

(5) Walker, N.; Stuart, D. *Acta Crystallogr.* 1983, A39, 158.

(6) Sheldrick, G. M. In *Crystallographic Computing 3*; Sheldrick, G. M., Kruger, C., Goddard, R., Eds.; Oxford University Press: Oxford, England, 1985; pp 175-189.

(7) Sheldrick, G. M. *SHELX-76. A Program for Crystal Structure Determination*, University of Cambridge: Cambridge, England, 1976.

(8) *International Tables for X-ray Crystallography*; Kynoch Press: Birmingham, England, 1974; Vol. IV, pp 99, 149.

(9) Schmidt, M. W.; Baldrige, K. K.; Boatz, J. A.; Jensen, J. H.; Koseki, S.; Gordon, M. S.; Nguyen, K. A.; Windus, T. L.; Elbert, S. T. *QCPE Bull.* 1990, 10, 52.

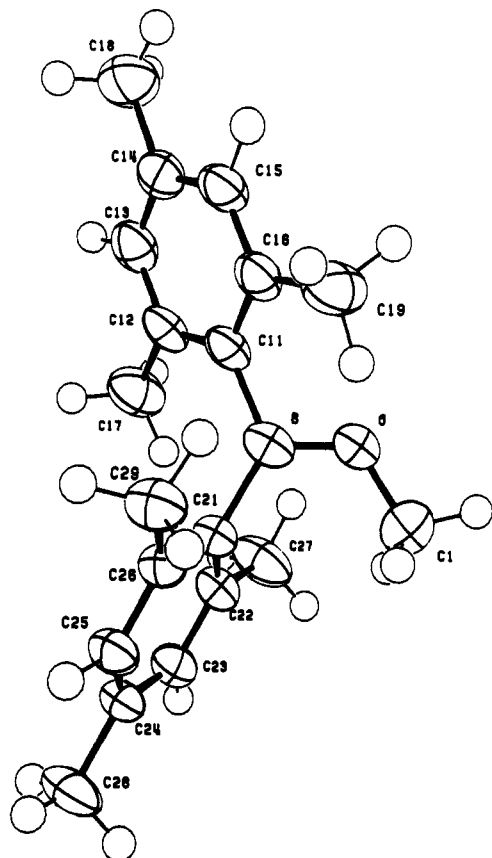


**Figure 1.** ORTEP drawing of  $(2,4,6\text{-C}_6\text{H}_2(\text{CH}_3)_3)_2\text{BOCH}_3$  ( $1(\text{X}=\text{O})$ ), showing the labeling scheme. Atoms are represented by thermal ellipsoids at the 90% level. Hydrogen atoms have been assigned arbitrary thermal parameters.

**Table 2.** Atomic Coordinates for  $(2,4,6\text{-C}_6\text{H}_2(\text{CH}_3)_3)_2\text{BOCH}_3$  ( $1(\text{X}=\text{O})$ )

atom	x	y	z
B	0.4408(4)	0.6110(4)	0.6652(3)
O	0.3508(3)	0.6910(2)	0.5756(2)
C1	0.3598(4)	0.8447(4)	0.5092(4)
C11	0.3958(4)	0.4457(3)	0.7373(3)
C12	0.5240(4)	0.3370(3)	0.7465(3)
C13	0.4788(4)	0.1929(3)	0.8058(3)
C14	0.3079(4)	0.1513(3)	0.8583(3)
C15	0.1813(4)	0.2582(3)	0.8523(3)
C16	0.2219(4)	0.4031(3)	0.7930(3)
C17	0.7147(4)	0.3702(4)	0.6874(4)
C18	0.2628(5)	-0.0055(4)	0.9166(4)
C19	0.0736(4)	0.5100(4)	0.7913(4)
C21	0.5733(4)	0.6854(3)	0.6946(3)
C22	0.7262(4)	0.7447(3)	0.5964(3)
C23	0.8382(4)	0.8134(3)	0.6234(3)
C24	0.8022(4)	0.8250(3)	0.7458(3)
C25	0.6511(4)	0.7659(3)	0.8435(3)
C26	0.5361(4)	0.6970(3)	0.8191(3)
C27	0.7778(4)	0.7332(4)	0.4611(3)
C28	0.9253(4)	0.9002(4)	0.7732(3)
C29	0.3705(4)	0.6393(3)	0.9266(3)

basis set is unnecessary since both yield essentially the same results. The d-orbital polarization exponents of Pople (the default values used in GAMESS) were used: B, 0.60; O, 0.80; S, 0.65. A H-B-X-H torsion angle was constrained during the structure optimizations of the stationary points on the conformational profile of  $2(\text{X}=\text{O},\text{S})$ . The GS and TS geometries of  $2(\text{X}=\text{O},\text{S})$  were constrained to  $C_s$  symmetry. Complete structure optimizations were performed on  $\text{H}_2\text{BXH-NH}_3$  ( $3(\text{X}=\text{O},\text{S})$ ).

(10) For hydrogen: Ditchfield, R.; Hehre, W. J.; Pople, J. A. *J. Chem. Phys.* 1971, 54, 724. For boron, nitrogen, and oxygen: Hehre, W. J.; Ditchfield, R.; Pople, J. A. *J. Chem. Phys.* 1972, 56, 2257. For sulfur: Francl, M. M.; Pietro, W.; Hehre, W. J.; Binkley, J. S.; Gordon, M. S.; DeFrees, D. J.; Pople, J. A. *J. Chem. Phys.* 1982, 77, 3654.

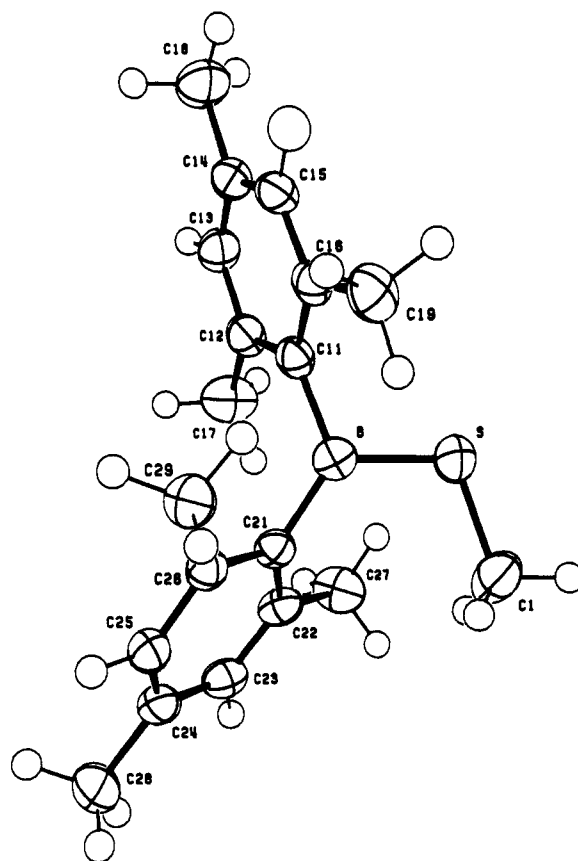


**Figure 2.** ORTEP drawing of  $(2,4,6\text{-C}_6\text{H}_2(\text{CH}_3)_3)_2\text{BSCH}_3$  ( $1(\text{X}=\text{S})$ ), showing the labeling scheme. Atoms are represented by thermal ellipsoids at the 45% level. Hydrogen atoms have been assigned arbitrary thermal parameters.

**Table 3.** Atomic Coordinates for  $(2,4,6\text{-C}_6\text{H}_2(\text{CH}_3)_3)_2\text{BSCH}_3$  ( $1(\text{X}=\text{S})$ )

atom	x	y	z
B	0.7444(4)	0.0276(7)	0.4818(4)
S	0.7216(1)	0.2169(2)	0.4254(1)
C1	0.7923(5)	0.3812(7)	0.4844(4)
C11	0.6894(4)	-0.1236(6)	0.4308(3)
C12	0.6160(4)	-0.2121(7)	0.4649(3)
C13	0.5618(4)	-0.3348(7)	0.4194(4)
C14	0.5769(4)	-0.3808(6)	0.3398(4)
C15	0.6512(4)	-0.2996(6)	0.3072(3)
C16	0.7062(4)	-0.1721(6)	0.3496(3)
C17	0.5925(5)	-0.1710(8)	0.5515(4)
C18	0.5137(5)	-0.5110(7)	0.2904(4)
C19	0.7826(4)	-0.0916(7)	0.3045(4)
C21	0.8104(3)	0.0122(6)	0.5723(3)
C22	0.7870(4)	0.0935(6)	0.6440(3)
C23	0.8457(4)	0.0672(7)	0.7233(3)
C24	0.9298(4)	-0.0345(6)	0.7343(3)
C25	0.9533(4)	-0.1100(6)	0.6634(3)
C26	0.8950(4)	-0.0920(6)	0.5838(3)
C27	0.6973(4)	0.2049(8)	0.6410(4)
C28	0.9928(5)	-0.0618(7)	0.8203(4)
C29	0.9260(4)	-0.1854(7)	0.5108(4)

## Results

**Crystal Structures.** The molecular structures of  $1(\text{X}=\text{O},\text{S};\text{R}=\text{CH}_3)$  consist of discrete, monomeric units. ORTEP drawings of  $1(\text{X}=\text{O},\text{R}=\text{CH}_3)$  and  $1(\text{X}=\text{S},\text{R}=\text{CH}_3)$  are given in Figures 1 and 2, respectively. Tables 2 and 3 give the final positional parameters for the non-hydrogen atoms of  $1(\text{X}=\text{O},\text{S};\text{R}=\text{CH}_3)$ , and Table 4 lists selected bond distances, bond angles, torsion angles, and angles between least-squares planes. Both compounds adopt approximate trigonal planar geometries, as indicated by the values and sums of the internal angles about the boron atoms of the oxygen ( $114.7 + 120.0 + 125.3 = 360.0^\circ$ ) and sulfur ( $112.2 + 123.8 + 124.0 = 360.0^\circ$ )

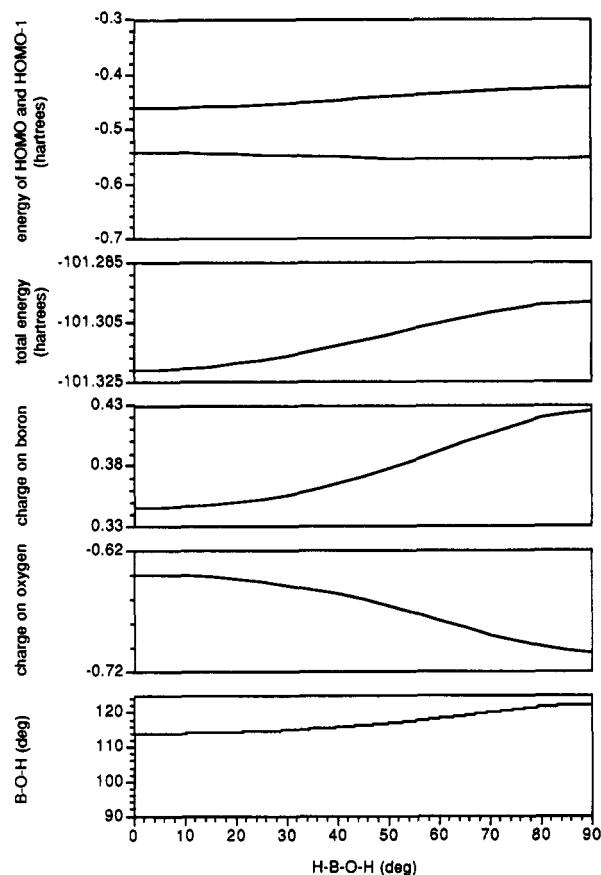


**Figure 3.** Summary of the results of the *ab initio* molecular orbital calculations on  $H_2BOH$  ( $2(X=O)$ ). The scales of the graphs are the same as the scales of the corresponding graphs of Figure 4. Note the HOMO is  $Bp\pi-Xp\pi$  and the HOMO-1 is  $Bp\pi-Xn\pi$ , opposite of the ordering found for  $2(X=S)$ .

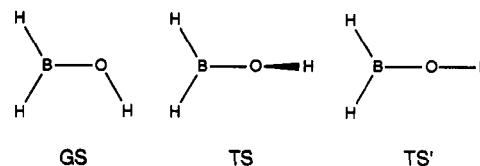
**Table 4.** Selected Bond Distances (Å), Bond Angles (deg), Torsional Angles (deg), and Dihedral Angles (deg) for  $(2,4,6-C_6H_2(CH_3)_3)_2BXCH_3$  ( $1(X=O,S)$ )

	X = O	X = S
Bond Distances		
B-X	1.352(5)	1.787(6)
B-C11	1.586(5)	1.592(8)
B-C21	1.584(5)	1.579(8)
X-C1	1.438(4)	1.815(6)
Bond Angles		
X-B-C11	114.7(3)	112.2(4)
X-B-C21	120.0(3)	124.0(4)
C11-B-C22	125.3(3)	123.8(5)
B-X-C1	123.6(3)	109.8(3)
Torsional Angles		
C1-X-B-C11	173.8(3)	-176.7(4)
C1-X-B-C21	-4.0(5)	3.9(6)
Dihedral Angles		
B/X/C11/C21-C11/C12/C13/	49.5(1)	60.8(2)
C14/C15/C16		
B/X/C11/C21-C21/C22/C23/	68.2(1)	60.6(2)
C24/C25/C26		

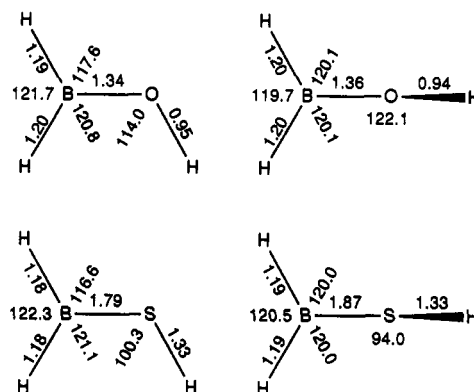
derivatives. The X-C moieties lie in the  $C_2BX$  planes, and the mesitylene rings are rotated  $\sim 60^\circ$  with respect to the  $C_2BX$  plane. Significant structural parameters for  $1(X=O,S;R=CH_3)$ : B-O = 1.351(5) Å, B-O-C = 123.6(3)°, C-B-O-C = 173.8(3)°, C'-B-O-C = -4.0(5)°; B-S = 1.792(6) Å, B-S-C = 109.4(3)°, C-B-S-C = 175.9(4)°, C'-B-S-C = -4.3(6)°.

**Molecular Orbital Calculations.** Previous *ab initio* studies have shown that the ground state (GS) structures of  $H_2BXH$  ( $2(X=O,S)$ ) exhibit  $C_s$  symmetry and coplanarity of all of the atoms. Thus, the two hydrogen atom substituents on the boron atom are chemically inequivalent. Topical exchange of these two hydrogen atoms can in principle take place via two distinct

mechanistic pathways, rotation about the B-X bond via transition state TS or inversion at X via transition state TS'.



The latter pathway for  $H_2BXH$  ( $2$ ) is 4.5 kcal mol<sup>-1</sup> higher in energy for X = O and 41.2 kcal mol<sup>-1</sup> higher in energy for X = S (at the RHF/6-31G\* level); therefore, we consider only rotation about the B-X bond here. Previous *ab initio* studies of the barriers to rotation about the B-X bonds of  $2(X=O,S)$  have employed a rigid rotation model in which only partial geometry optimizations of the ground-state and transition-state structures were performed.<sup>11</sup> Such calculations give an upper limit to the barriers to rotation about the B-X bonds of  $2$ . A complete investigation of the energy variation accompanying a conformational change requires relaxation of all the other molecular coordinates.<sup>12</sup> The present calculations are at the RHF/6-31G\* level with complete geometry optimization (with the exception of a H-B-X-H torsion angle) in  $5^\circ$  intervals of the rotation coordinate. Electron correlation was not considered.<sup>13</sup> The results of our calculations are summarized in Figures 3 and 4. The optimized GS and TS geometries for  $2$  are as follows:



The  $BH_2$  moieties of  $2$  are largely unaffected by rotation about the B-X bond. In contrast, the B-X distances and B-X-H angles vary markedly. The B-X distance increases 0.08 Å (4.5%), whereas the B-O distance only increases 0.02 Å (1.5%) upon rotation from the  $C_s$  ground-state conformer to the  $C_s$  transition-state conformer. Furthermore, the B-O-H angle increases  $8.1^\circ$  whereas the B-S-H angle decreases  $6.3^\circ$  in going from the ground- to the transition-state orientation. The barrier to rotation about the B-X bond of  $H_2BXH$  calculated at the RHF/6-31G\* level is 14.3 kcal mol<sup>-1</sup> for X = O and 18.0 kcal mol<sup>-1</sup> for X = S.

(11) (a) Gropen, O.; Nilssen, E. W.; Seip, H. M. *J. Mol. Struct.* 1974, 23, 289. (b) Gropen, O.; Johansen, R. *J. Mol. Struct.* 1975, 25, 161. (c) Dill, J. D.; Schleyer, P. v. R.; Pople, J. A. *J. Am. Chem. Soc.* 1975, 97, 3402.

(12) (a) *Internal Rotation in Molecules*; Orville-Thomas, W. J., Ed.; Wiley: New York, 1974. (b) Payne, P. W.; Allen, L. C. In *Modern Theoretical Chemistry*; Schaefer, H. F., Ed.; Plenum Press: New York, 1977, Vol. 4, p 29. (c) Lister, D. G.; Macdonald, J. N.; Owen, N. L. *Internal Rotation and Inversion*; Academic Press: London, 1978. (d) Hehre, W. J.; Radom, L.; Schleyer, P. v. R.; Pople, J. A. *Ab Initio Molecular Orbital Theory*; Wiley: New York, 1986; Section 6.4, p 261.

(13) At the suggestion of a reviewer, we have optimized the GS and TS structures of  $2(X=O,S)$  at the MP2/6-31G\* level. The geometries are not affected significantly. As expected however, the rotational barriers increase when electron correlation is taken into account, becoming 17.0 kcal mol<sup>-1</sup> for X = O and 21.4 kcal mol<sup>-1</sup> for X = S. The conclusions of this paper are not affected by the results of the MP2/6-31G\* calculations since the rotational barrier for X = S is still larger than that calculated for X = O. Also at the suggestion of the reviewer, we have carried out "two-configuration self-consistent-field" (TCSCF) calculations on the TS geometries of  $2(X=O,S)$ . As expected, given the difference in electronegativities of the atoms of the heteronuclear bond, no diradical character is observed.

## Discussion

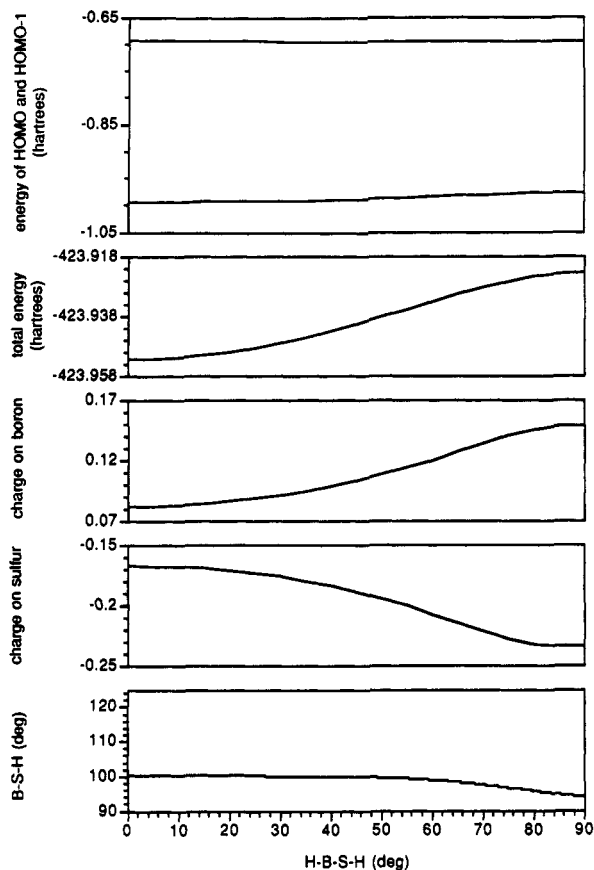
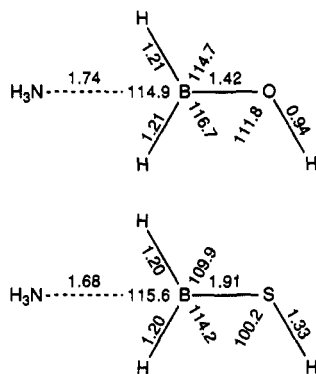


**Figure 4.** Summary of the results of the *ab initio* molecular orbital calculations on  $H_2BSH$  ( $2(X=S)$ ). The scales of the graphs are the same as the scales of the corresponding graphs of Figure 3. Note the HOMO is  $Bp\pi-Xn\pi$  and the HOMO-1 is  $Bp\pi-Xp\pi$ , opposite of the ordering found for  $2(X=O)$ .

The molecular structures of  $H_2BXH\cdot NH_3$  ( $3(X=O,S)$ ), which may be viewed as coordinatively saturated derivatives of **2**, were also investigated. The resulting geometries are summarized as follows:



Interestingly, the  $H_2BXH$  moieties of **3** retain some of the trigonal planar character of **2**, as indicated by the values and sums of the corresponding H-B-H and H-B-X angles of the oxygen ( $114.7 + 114.9 + 116.7 = 346.3^\circ$ ) and sulfur ( $109.9 + 114.2 + 115.6 = 339.7^\circ$ ) derivatives. Furthermore, the conformations about the B-X bonds of **3** with respect to the "trigonal" planes of the  $H_2BX$  moieties are related to the GS conformations of **2**, as indicated by the N-B-X-H torsion angles of the oxygen ( $105.0^\circ$ ) and sulfur ( $85.9^\circ$ ) derivatives. With respect to the GS geometries of **2**, the most significant change in the  $H_2BXH$  moieties of **3** occurs in the B-X bond lengths, which are elongated by  $0.08 \text{ \AA}$  (6%) for  $X = O$  and  $0.12 \text{ \AA}$  (6%) for  $X = S$ . The long B-N bond lengths suggest that the  $NH_3$  groups are relatively weakly bound to the boron atom of **3**. The  $H_2BX$  and  $NH_3$  groups adopt staggered conformations about the B-N bond.

Surprisingly little is known about the molecular structures of coordinatively unsaturated borates and thioborates. A search of the Cambridge Structural Database (V4.60) produced only two examples of structurally characterized organoborates of the type  $R_2BOR'$ : phenyl(tris(trimethylsilyl)methyl)(5,5,5-tris(trimethylsilyl)pentoxy)borane,<sup>14</sup> which bears sterically demanding substituents at the boron and oxygen atoms, and diphenylborinic acid,<sup>15</sup> which cocrystallizes with a disordered borane and bears a hydrogen atom substituent that is involved in intermolecular hydrogen bonding. No examples of organothioborates of the type  $R_2BSR'$  have been structurally characterized by X-ray crystallography.<sup>16</sup> Therefore, the structures of  $1(X=O, R=CH_3)$  and  $1(X=S, R=CH_3)$  represent the first opportunity to compare the molecular structures of a pair of coordinatively unsaturated boranes that contain a single  $XR \pi$ -donor group and the same, relatively innocent ancillary substituents. The ORTEP drawings of  $1(X=O, R=CH_3)$  and  $1(X=S, R=CH_3)$  in Figures 1 and 2 show the two compounds exhibit comparable molecular structures. Table IV compares selected structural features of  $1(X=O, S; R=CH_3)$ . Both compounds adopt approximate trigonal planar geometries (*vide supra*). The  $XCH_3$  moieties lie in the  $C_2BX$  planes, an orientation about the B-X bond that maximizes  $Bp\pi-Xp\pi$  bonding (*vide infra*). The mesitylene rings are rotated approximately  $60^\circ$  with respect to the  $C_2BX$  plane, which prohibits significant  $Bp\pi$ -aryl interaction. We note here that the solid-state structures of **1** refute the conclusion of Davidson *et al.*<sup>3d</sup> that one of the mesitylene rings of **1** is coplanar with the  $C_2BX$  plane in solution. The crystal structures of  $1(X=O, S)$  offer a benchmark for comparing discrete  $Bp\pi-Xp\pi$  bonds. We now consider, in light of these crystal structures and the *ab initio* calculations that have been carried out to complement them, the three factors that have been cited as evidence of  $p\pi-p\pi$  bonding in  $R_2BXR'$  compounds: (1) short B-X bond distances, (2) relatively large B-X-R' bond angles, and (3) significant rotational barriers about the B-X bonds.

**B-X Bond Lengths and  $Bp\pi-Xp\pi$  Bonding.** Naturally, the B-X bond lengths should reflect the significance of  $Bp\pi-Xp\pi$  bonding. But, what constitutes a "normal" B-X single-bond length? We will consider several interpretations of this issue.

It is possible to calculate the "effective radii" of the B and X atoms by assuming the B-C and X-C interatomic distances represent single bonds with  $r_H = 0.32 \text{ \AA}$  and  $r_C = 0.77 \text{ \AA}$ .<sup>17</sup> For  $1(X=O, R=CH_3)$ :  $r_B = 1.58 - 0.77 = 0.81 \text{ \AA}$  and  $r_O = 1.44 - 0.77 = 0.67 \text{ \AA}$ . The observed B-O distance ( $1.35 \text{ \AA}$ ) is  $0.13 \text{ \AA}$  shorter (9%) than the predicted distance, which is given by  $r_B + r_O = 0.81 + 0.67 = 1.48 \text{ \AA}$ . For  $1(X=S, R=CH_3)$ :  $r_B = 1.58 - 0.77 = 0.81 \text{ \AA}$  and  $r_S = 1.82 - 0.77 = 1.05 \text{ \AA}$ . The observed B-S distance ( $1.79 \text{ \AA}$ ) is  $0.07 \text{ \AA}$  shorter (3%) than the predicted distance, which is given by  $r_B + r_S = 0.81 + 1.05 = 1.86 \text{ \AA}$ . We have assumed that the B-X bond is covalent in this analysis of the B-X bond lengths. The difference in electronegativity between

(14) Eaborn, C.; Retta, N.; Smith, J. D.; Hitchcock, P. B. *J. Organomet. Chem.* 1982, 235, 265.

(15) Rettig, S. J.; Trotter, J. *Can. J. Chem.* 1983, 61, 2334.

(16) The structure of  $Me_2BSMe$  has been determined in the gas-phase by electron diffraction: Brendhaugen, K.; Wisløff Nilssen, E.; Seip, H. M. *Acta Chem. Scand.* 1973, 27, 2965. Johansen, R.; Seip, H. M.; Siebert, W. *Acta Chem. Scand.* 1975, A29, 644.

(17) Calculated for ethane:  $r_C = d_{CC}/2 = 1.54/2 = 0.77 \text{ \AA}$ . Calculated for methane:  $r_H = d_{CH} - r_C = 1.09 - 0.77 = 0.32 \text{ \AA}$ .

B and X should be taken into account if the B–X bond possesses a significant ionic component.

Of the many models that have been proposed to account for ionic contributions to bond lengths, we consider here the Schomaker–Stevenson formula as modified by Haaland:<sup>18</sup>

$$d(\text{A–B}) = r_{\text{A}} + r_{\text{B}} - c|\chi_{\text{A}} - \chi_{\text{B}}|^n; \quad c = 0.085 \text{ \AA}, \quad n = 1.4$$

where  $r_{\text{A}}$  and  $r_{\text{B}}$  and  $\chi_{\text{A}}$  and  $\chi_{\text{B}}$  are the radii and electronegativities of atoms A and B, respectively. The Schomaker–Stevenson–Haaland formula was used recently to interpret the bond lengths observed for organoaluminum compounds of the type  $\text{R}_2\text{AlOR}$ .<sup>19</sup> Using Allred–Rochow electronegativities and the covalent radii of Haaland, the B–O bond distance calculated for the GS geometry of  $2(\text{X}=\text{O})$  using the Schomaker–Stevenson–Haaland formula (1.38 Å) is comparable to the distance observed in  $1(\text{X}=\text{O}, \text{R}=\text{CH}_3)$  (1.351(5) Å). The calculated and observed GS distances for  $2(\text{X}=\text{S})$  (1.81 Å) and  $1(\text{X}=\text{S}, \text{R}=\text{CH}_3)$  (1.792(6) Å) are also comparable. Although the observed bond lengths are shorter than the lengths predicted using the Schomaker–Stevenson–Haaland formula and the ratio of the observed/calculated B–O distances is proportionally larger than the ratio of the observed/calculated B–S distances, the difference is not as great (X = O, 2%; X = S, 1%). But does the Schomaker–Stevenson–Haaland formula predict B–X single-bond lengths, or is it biased toward predicting a typical bond length? Since the parameters of the empirical Schomaker–Stevenson–Haaland formula are based upon a least-squares fit of actual compounds, within the limitations of the scope of the compounds investigated, the equation predicts a typical bond length. Only 3-coordinate trivalent boron compounds (e.g.  $\text{BX}_3$ ; X =  $\text{CH}_3$ ,  $\text{NHCH}_3$ ,  $\text{OCH}_3$ ,  $\text{SCH}_3$ , F, Cl, Br, I) were considered by Haaland; accordingly, the calculated atomic radius of boron was determined for coordinatively unsaturated compounds, many of which bear groups that are capable of  $\pi$  donation. Such compounds are expected to exhibit some degree of multiple bonding. This is reflected in the fact that the Schomaker–Stevenson–Haaland formula tends to do a poor job in predicting homoatomic bond lengths (e.g.:  $d(\text{H–H})_{\text{obs}} = 0.74$ ,  $d(\text{H–H})_{\text{calc}} = 0.68$ ;  $d(\text{H}_2\text{B–BH}_2)_{\text{obs}} = 1.77$ ,  $d(\text{B–B})_{\text{calc}} = 1.62$ ;  $d(\text{HO–OH})_{\text{obs}} = 1.48$ ,  $d(\text{O–O})_{\text{calc}} = 1.44$ ;  $d(\text{HS–SH})_{\text{obs}} = 2.05$ ,  $d(\text{S–S})_{\text{calc}} = 2.06$ ). In most cases for homoatomic bonds, the calculated bond length is shorter than the observed bond length, which suggests the ionic contribution to the bond lengths calculated using the Schomaker–Stevenson–Haaland formula are overemphasized. Table 5 summarizes the B–X bond distances that are calculated using these two models and compares the computed values with those that have been measured experimentally. We believe the first approach, calculation of effective radii, presents a clearer picture of the multiple-bond character of the B–X bonds in 1. On this point, we note that three crystal structures<sup>15</sup> of coordinatively saturated organoborates of the formula  $\text{Ph}_2\text{BO}(\text{CH}_2)_n\text{NR}_2$  (4) exhibit B–O bond lengths that are elongated with respect to  $1(\text{X}=\text{O}, \text{R}=\text{H})$ :  $\text{B–O}_{\text{avg}} = 1.477(5)$  Å, which happens to be exactly the value predicted above for a B–O single bond using the effective radii model!

For the sake of comparison with the results obtained from the crystallographic study, let us calculate the

Table 5. Calculated and Observed B–X Bond Distances (Å)

	calcd single-bond length		obsd <sup>c</sup>
	SSH <sup>a</sup>	effective radii <sup>b</sup>	
H <sub>2</sub> BOH	1.38	1.51	1.34
Ph <sub>2</sub> BOH	1.38		1.348(3)
Mes <sub>2</sub> BOMe	1.38	1.48	1.351(5)
H <sub>2</sub> BOH·NH <sub>3</sub>	1.38	1.51	1.42
Ph <sub>2</sub> BO(CH <sub>2</sub> ) <sub>3</sub> NH <sub>2</sub>	1.38	1.51	1.478(2)
Ph <sub>2</sub> BO(CH <sub>2</sub> ) <sub>2</sub> NH <sub>2</sub>	1.38	1.46	1.482(3)
Ph <sub>2</sub> BO(CH <sub>2</sub> ) <sub>2</sub> NMe <sub>2</sub>	1.38	1.50	1.470(2)
H <sub>2</sub> BSH	1.81	1.87	1.79
Mes <sub>2</sub> BMe	1.81	1.86	1.792(6)
H <sub>2</sub> BSH·NH <sub>3</sub>	1.81	1.89	1.91

<sup>a</sup> Calculated using the Schomaker–Stevenson formula as modified by Haaland. <sup>b</sup> Assumes  $r_{\text{H}} = 0.32$  Å and  $r_{\text{C}} = 0.77$  Å and the B–C and X–C bond lengths represent single bonds. <sup>c</sup> Bond distances with errors are from X-ray crystal structures, and those without are from *ab initio* calculations.

effective radii of the B and X atoms of 2 by assuming the B–H and X–H interatomic distances represent single bonds and  $r_{\text{H}} = 0.32$  Å.<sup>17</sup> For  $2(\text{X}=\text{O})$ :  $r_{\text{B}} = 0.87$  Å and  $r_{\text{O}} = 0.63$  Å. The B–O distance obtained from the *ab initio* molecular orbital calculations (1.34 Å) is 0.16 Å shorter (11%) than the distance predicted using the Schomaker–Stevenson–Haaland formula (1.51 Å). For  $2(\text{X}=\text{S})$ :  $r_{\text{B}} = 0.86$  Å and  $r_{\text{S}} = 1.01$  Å. The B–O distance obtained from the *ab initio* molecular orbital calculations (1.79 Å) is 0.08 Å shorter (4%) than the sum of the effective radii (1.87 Å). The B–O and B–S distances calculated quantum chemically are 2.9% and 1.3% shorter than the distances calculated using the Schomaker–Stevenson–Haaland formula. As expected, the B–X bond distance lengthens in the corresponding coordinatively saturated species 3. The B–O distance increases from 1.34 to 1.42 Å (6%), and the B–S distance increases from 1.79 to 1.91 Å (7%). Although the sum of the effective radii of B and S (1.89 Å) agrees well with the bond length observed for  $3(\text{X}=\text{S})$  (1.91 Å), the sum of the effective radii of B and O (1.51 Å) is substantially greater than the bond length observed for  $3(\text{X}=\text{O})$  (1.42 Å). However, this is consistent with the substantially longer B–N distance obtained for  $3(\text{X}=\text{O})$  (1.74 Å) as compared to the B–N distance obtained for  $3(\text{X}=\text{S})$  (1.68), which suggests that the alkoxide group is a better donor than the sulfur group. This is further indicated by the geometry about the  $2(\text{X}=\text{O})$  moiety of  $3(\text{X}=\text{O})$ , which is much more like the ground-state structure of 2 than the  $2(\text{X}=\text{S})$  moiety of  $3(\text{X}=\text{S})$ ; *vide supra*.

The above analysis of bond lengths of 1–4 using the effective radii model suggests that the B–O bond is comparatively stronger than the B–S bond in 1. Furthermore, since the bond dissociation energy of the O–H bond in H<sub>2</sub>O is 118.0 kcal mol<sup>-1</sup> and that of the S–H bond<sup>20</sup> in CH<sub>3</sub>SH is 89.0 kcal mol<sup>-1</sup>, the fact that  $1(\text{X}=\text{S}, \text{R}=\text{CH}_3)$  is readily hydrolyzed to give  $1(\text{X}=\text{O}, \text{R}=\text{H})$  also speaks to the greater strength of the B–O bond as compared to the B–S bond. Of course, the lengths and the dissociation energies of the B–X bonds reflect the combined strength of the  $\sigma$  and  $\pi$  bonds. We will consider later the question of the relative  $\pi$ -donor abilities of the alkoxide and thiolate groups toward the R<sub>2</sub>B  $\pi$  acceptor.

**B–X–R Bond Angles and Bp $\pi$ –Xp $\pi$  Bonding.** Rothwell *et al.* have concluded that M–O–R bond angles vary substantially when M is a transition metal, but M–O–R angles are not reliable indicators of M–O  $\pi$ -bond

(18) (a) Schomaker, V.; Stevenson, D. P. *J. Am. Chem. Soc.* 1941, 63, 37. (b) Blom, R.; Haaland, A. *J. Mol. Struct.* 1985, 128, 21.

(19) Petrie, M. A.; Olmstead, M. M.; Power, P. P. *J. Am. Chem. Soc.* 1991, 113, 8704.

(20) Shum, L. G. S.; Benson, S. W. *Int. J. Chem. Kinet.* 1985, 17, 277.

strengths.<sup>21</sup> Furthermore, M.T.A. has concluded that, aside from those cases that involve sterically demanding substituents, M-S-R bond angles do not vary with M.<sup>22</sup> Obtuse Al-O-R bond angles in both coordinatively unsaturated 3-coordinate and coordinatively saturated 4-coordinate aluminum alkoxides have been attributed to electronic factors,<sup>23</sup> although steric factors are also important.<sup>24</sup> The Al-O bond in such compounds has been described as largely ionic.<sup>19</sup> In this regard we note that the gas-phase structure of the ionic alkaline earth monohydroxide free radical complex Ca<sup>+</sup>OH is linear, but the corresponding Ca<sup>+</sup>SH complex exhibits a bent structure.<sup>25</sup> The former has been described as ionic; the latter, as more covalent.<sup>26</sup>

The corresponding B-X-R bond angles in 1(X=O,S;R=CH<sub>3</sub>) and 2(X=O,S) are markedly different: B-O-H = 114.0°, B-O-CH<sub>3</sub> = 123.6(3)°, B-S-H = 100.3°, B-S-CH<sub>3</sub> = 109.4(3)°. In both cases, the angle observed for 1(X=O,S;R=CH<sub>3</sub>) is larger (by ca. 10°) than the angle calculated for 2(X=O,S). This can be attributed to the greater steric demand of the methyl group as compared to the hydrogen atom. The latter steric effect is also suggested by the fact that the B-O-H angle *increases* 8.1° whereas the B-S-H angle *decreases* 6.3° in going from the GS to the TS orientation. The B-O-H angle increases as a result of an effort to stabilize the TS geometry of 2(X=O) through  $\pi$  donation (*vide infra*); the decrease in the B-S-H angle may be attributed to a relief of Pauli repulsion between the BH and SH groups in going from the GS to the TS structure. These trends are consistent with those involving transition metals for which the M-O-R bond angles of transition metal-alkoxide complexes depend upon both the electron requirements of M and steric factors, whereas the M-S-R bond angles of transition metal-thiolate complexes are only influenced by steric factors.

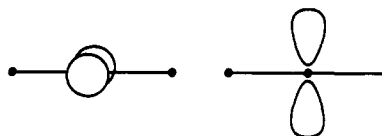
**Rotational Barriers about the B-X Bond and B $\pi$ -X $\pi$  Bonding.** The barriers to rotation about the B-X bonds of H<sub>2</sub>BXH calculated at the RHF/6-31G\* level are 14.3 kcal mol<sup>-1</sup> for X = O and 18.0 kcal mol<sup>-1</sup> for X = S. These calculated barriers compare favorably with the value of 13.2 kcal mol<sup>-1</sup> that has been measured for 1(X=O,R=CH<sub>3</sub>)<sup>3a</sup> and the value of 18.4 kcal mol<sup>-1</sup> that has been measured for 1(X=S,R=C<sub>6</sub>H<sub>5</sub>).<sup>3c</sup> Remarkably, the barrier to rotation about the B-S bond is substantially greater than the related barrier to rotation about the B-O bond. This has led some workers to the surprising conclusion that the thiolate ligand is a better  $\pi$  donor compared to the alkoxide in this particular system. This implies that the B2 $\pi$ -S3p $\pi$  bond is stronger than the B2p $\pi$ -O2p $\pi$  bond. We have carried out *ab initio* molecular orbital calculations on the model systems 2 in an effort to address this counterintuitive result.

The BH<sub>2</sub> moiety is a *single-sided*  $\pi$  acceptor; therefore, we should attempt to compare the single-sided donor

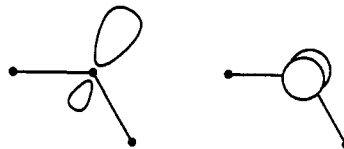
abilities of OH and SH. In contrast to the single-sided nature of the  $\pi$ -acceptor BH<sub>2</sub> group, XH groups may in principle serve as double-sided  $\pi$  donors. The extent to which this is possible depends on the geometry of the XH group. If strongly bent, the XH group serves as a single-sided  $\pi$  donor, with one Xp orbital serving as the  $\pi$ -donor orbital; the in-plane orbital would be largely Xs in character and would, therefore, possess the wrong symmetry to mix with the Bp $\pi$  acceptor orbital



and if linear, the XH group serves as a double sided  $\pi$  donor, with two Xp orbitals serving as the  $\pi$ -donor orbitals



In reality, the GS and TS geometries of 2 lie somewhere between these limiting cases where the out-of-plane donor orbital consists of a Xp orbital and the in-plane donor orbital possesses both Xs and Xp character:



We consider first the GS geometries of 2 wherein the  $\pi$  bond is composed of effectively discrete Bp<sub>z</sub> and Xp<sub>z</sub> orbitals. Accordingly, the relative contributions of the B and X orbitals to the B-X  $\pi$  bond can be assessed by analysis of the Mulliken populations. Indeed, this is one of the principal reasons that we undertook this study, for the GS geometries allow us to test the relative single-sided  $\pi$ -donor abilities of the OH and SH groups with regard to the BH<sub>2</sub>  $\pi$  acceptor. For the GS geometry, the Mulliken populations of the Bp<sub>z</sub> and the Xp<sub>z</sub> orbitals for 2(X=O) are 0.182 and 1.978. The corresponding populations for 2(X=S) are 0.182 and 1.994. According to the Mulliken populations, it would seem that the OH and SH groups are comparable single-sided  $\pi$  donors with regard to the BH<sub>2</sub>  $\pi$  acceptor. In contrast for the corresponding TS geometries, the Mulliken populations of the Bp<sub>z</sub> orbitals of the oxygen and sulfur derivatives are 0.107 and 0.049. This represents a 40% reduction in  $\pi$  donation for 2(X=O) and a 73% reduction for 2(X=S). Accordingly, the OH group is a better  $\pi$  donor than the SH group in the TS geometry of 2.

The trend in B-X distances reflects the greater relative stability of the rotational transition state of the oxygen analogue as compared to the sulfur derivative. The trends in the angles reflect a relief of Pauli repulsion in the case of the sulfur derivative and an effort to mix more O2s character into the in-plane lone pair of the oxygen derivative so as to improve overlap with the B2p<sub>z</sub> acceptor orbital. These geometry changes support our view that the thiolate is effectively a *single-sided* (2-electron)  $\pi$ -donor group whereas the alkoxide is capable to some extent of serving as a *double-sided* (4-electron)  $\pi$ -donor group:

(21) Coffindaffer, T. W.; Steffy, B. D.; Rothwell, I. P.; Foltling, K.; Huffman, J. C.; Streib, W. E. *J. Am. Chem. Soc.* 1989, 111, 4742

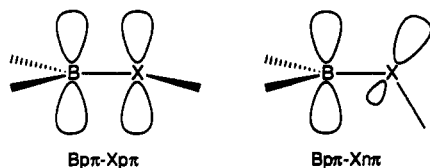
(22) Ashby, M. T. *Comments Inorg. Chem.* 1990, 10, 297.

(23) Barron, A. R.; Dobbs, K. D.; Francl, M. M. *J. Am. Chem. Soc.* 1991, 113, 39.

(24) Healy, M. D.; Ziller, J. W.; Barron, A. R. *Organometallics* 1991, 10, 597.

(25) Bernath, P. F. *Science* 1991, 254, 665.

(26) See also for ( $\eta^5$ -C<sub>5</sub>R<sub>5</sub>)M<sup>II</sup>(NO)(XR)<sub>2</sub> (M = Cr, X = O; M = Mo, X = S) and related transition metal systems, where M is a single-sided  $\pi$  acceptor and XR a single-sided  $\pi$  donor: Ashby, M. T.; Enemark, J. H. *J. Am. Chem. Soc.* 1986, 108, 730. Hubbard, J. L.; McVicar, W. K. *Inorg. Chem.* 1992, 31, 910. For R<sub>2</sub>PNR', where R<sub>2</sub>P is a  $\pi$  acceptor and NR' is a single-sided  $\pi$  donor: Ashby, M. T.; Li, Z. *Inorg. Chem.* 1992, 31, 1321. Trinquie, G.; Ashby, M. T. *Inorg. Chem.*, in press.



That is, whereas the  $Bp\pi-Xp\pi$  bonding interaction is important for both  $X = O$  and  $S$ , the  $Bp\pi-Xn\pi$  interaction is only significant for  $X = O$  (see the energies of the HOMO and HOMO-1 in Figures 3 and 4). Importantly, the  $Bp\pi-Xp\pi$  interaction, the stronger of the two  $\pi$  bonds, does not depend on the  $B-X-R$  bond angle. Therefore, when the  $XR$  group is bound to a single-sided  $\pi$  acceptor such as  $R_2B$ , the  $B-X-R$  bond angle is not an indicator of the degree of  $B-X$   $\pi$  bonding when the orientation favors  $Bp\pi-Xp\pi$  bonding (except to the extent that Pauli repulsions may be reduced, thereby allowing shorter  $B-X$  bond distances and better  $Bp\pi-Xp\pi$  overlap). Of course, the  $B-X-R$  angle is significant when the orientation favors  $Bp\pi-Xn\pi$  bonding.

**Relationship between  $\pi$ -Bond Strength and Rotational Barriers.** Perhaps the simplest definition of the strength a  $\pi$  bond of a doubly-bonded species  $X=Y$  is the activation energy associated with rotation about the  $X=Y$  bond.<sup>1b</sup> However, the latter definition is only tenable if (1) the  $X=Y$  bond length does not change during the rotation (the  $\sigma$  bond will be affected if the bond length changes), (2) steric interactions are not important or are at least counterbalanced, and (3) the  $\pi$  interaction between  $X$  and  $Y$  is completely eliminated in the rotational transition-state geometry. If only the last condition is not met, the activation energy for rotation about the  $X=Y$  bond represents the *difference* between the two  $X=Y$   $\pi$ -bonding interactions, not the strength of the  $X=Y$   $\pi$  bond. The limitation of using rotational barriers as a measure of  $\pi$ -bond strengths has been discussed previously.<sup>1b</sup>

The in-plane lone pair of the  $OH$  group is a substantially better donor to the  $BH_2$  acceptor orbital than the in-plane lone pair of the  $SH$  group. Since the latter donation has a stabilizing effect,  $2(X=O)$  in the TS geometry is closer in energy to  $2(X=O)$  in the GS geometry than the corresponding sulfur derivative. Since the barrier to rotation corresponds to the difference in the energies of the GS and TS structures, that barrier is smaller for the oxygen derivative than for the sulfur derivative, despite the fact that both derivatives are comparable single-sided  $\pi$  donors and the oxygen derivative is a substantially better double-sided donor than the sulfur compound. It is clear that the rotational barriers about the  $X=Y$  bonds of compounds for which  $X$  are single-sided  $\pi$ -acceptor groups and  $Y$  are bent double-sided  $\pi$ -donor groups are not measures of the relative  $\pi$ -bond strengths.<sup>27</sup>

**Origin of the Differences in  $M-OR$  and  $M-SR$   $\pi$ -Bonding.** Why does the  $OH$  group of  $H_2BOH$  stabilize the perpendicular transition state more effectively than the  $SH$  group of  $H_2BSH$ ? I.e., why does the alkoxide group serve as a more effective double-sided  $\pi$  donor relative to the thiolate group? There is apparently an increased propensity for the  $2s$  and  $2p$  orbitals of oxygen to mix as compared to the  $3s$  and  $3p$  orbitals of sulfur. This trend

is particularly curious given the fact the  $3s$  and  $3p$  orbitals of atomic sulfur are closer in energy than the  $2s$  and  $2p$  orbitals of atomic oxygen.<sup>27</sup> Kutzelnigg has discussed the fact that both lone-pair repulsion and isovalent hybridization play a greater role for the lighter main group elements than for the heavier main group elements.<sup>2</sup> The essential difference between the elements of the first row and those of the higher rows is that the core of the former consists of only an  $s$  orbital, whereas the core of the latter consists of  $s$ ,  $p$ , and in some cases  $d$  orbitals. As a result of this the valence  $s$  and  $p$  orbitals of the first row elements exhibit similar effective radii, whereas the valence  $p$  orbitals of the heavier elements exhibit larger effective radii than their valence  $s$  orbitals. Accordingly, the  $2s$  and  $2p$  orbitals of oxygen overlap to a larger extent than the  $3s$  and  $3p$  orbitals of sulfur. These overlap considerations apparently outweigh the unfavorable energy separation of the  $O$   $2s$  and  $2p$  orbitals relative to the  $S$   $3s$  and  $3p$  orbitals. As an aside, if the  $2s$  and  $2p$  orbitals of oxygen mix more readily than the  $3s$  and  $3p$  orbitals of sulfur, this should be reflected in a higher *inversion* barrier for  $H_2BSH$  as compared to  $H_2BOH$ . The energy difference between the GS and linear ( $C_{2v}$ ) structures of  $H_2BXH$  (2) at the RHF/6-31G\* level is only  $14.3 \text{ kcal mol}^{-1}$  for  $X = O$ , but the energy difference is  $59.2 \text{ kcal mol}^{-1}$  for  $X = S$ !

## Conclusions

We conclude that the  $OR'$  and  $SR'$  groups are comparable  $\pi$  donors in the ground-state geometry of  $R_2BXR'$  ( $R-B-X-R' = 0^\circ$ ), but the  $OR'$  group is a much better  $\pi$  donor than the  $SR'$  group in the transition state geometry of  $R_2BXR'$  ( $R-B-X-R' = 90^\circ$ ). Thus the larger barrier to rotation observed for the sulfur derivative relative to the oxygen derivative of  $R_2BXR'$  is attributed to a greater stabilization of the transition state by oxygen and not a stronger  $Bp\pi-Sp\pi$  bond in the ground state. Accordingly, the rotational barriers about the  $B-X$  bonds of  $R_2BXR'$  are not measures of the relative  $B-X$   $\pi$  bond strengths. The difference in the spatial nature of the alkoxide and thiolate donor orbitals may be attributed to the increased propensity for the  $2s$  and  $2p$  orbitals of oxygen to mix as compared to the  $3s$  and  $3p$  orbitals of sulfur. In effect, alkoxide ligands are capable of serving as double-sided  $\pi$  donors whereas thiolates are single-sided  $\pi$  donors. This should be borne in mind when one compares their relative donor abilities.

**Acknowledgment** is made to the donors of the Petroleum Research Fund, administered by the American Chemical Society, for partial support of this research. M.T.A. thanks the University of Oklahoma for a Junior Faculty Summer Research Fellowship. We thank Dr. M. W. Schmidt for providing us with a current version of GAMESS and Prof. P. P. Power for sharing results prior to publication.

**Supplementary Material Available:** Listings of anisotropic thermal parameters and bond distances and angles (4 pages). Ordering information is given on any current masthead page.

OM930600P

(27) Moore, C. E. *Atomic Energy Levels*, National Bureau of Standards: Washington, DC, 1949.